Antitumor Polycyclic Acridines. 20.[1] Search for DNA Quadruplex Binding Selectivity in a Series of 8,13-Dimethylquino[4,3,2-*kl*]acridinium Salts: Telomere- Targeted Agents

Mai-Kim Cheng,[†] Chetna Modi,[†] Jennifer C. Cookson,[†] Ian Hutchinson,[†] Robert A. Heald,[†] Andrew J. McCarroll,[†] Sotiris Missailidis,[#] Farial Tanious,[‡] W. David Wilson,[‡] Jean-Louis Mergny,[§] Charles A. Laughton,[†] and Malcolm F. G. Stevens*[,†]

Cancer Research U.K. Experimental Cancer Chemotherapy Research Group, Centre for Biomolecular Sciences, School of Pharmacy, University of Nottingham, Nottingham NG7 2RD, U.K., Chemistry Department, The Open University, Walton Hall, Milton Keynes MK7 6AA, U.K., Department of Chemistry, Georgia State University, Atlanta, Georgia 30303, and Laboratoire de Biophysique, INSERM U565, CNRS UMR5153, Museum National d'Histoire Naturelle, 43 Rue Cuvier, 75005 Paris, France

Received May 21, 2007

The growth-inhibitory activities of an extensive series of quaternized quino[4,3,2-*kl*]acridinium salts against tumor cell lines in vitro have been measured and their biological properties interpreted in the light of differential binding to different DNA isoforms. Selectivity for quadruplex DNA binding and stabilization by compounds were explored through an array of methods: UV absorption and fluorescence emission spectroscopy, surface plasmon resonance, and competition dialysis. Quadruplex DNA interaction was further characterized through FRET and DNA polymerase arrest assays. Telomerase inhibition, inferred from the TRAP assay, is attributed to quadruplex stabilization, supported by the strong correlation ($R^2 = 0.81$) across the series between quadruplex DNA binding affinity and TRAP inhibition potency. Growth inhibition potency in the NCI60 human tumor cell line panel is more marked in compounds with greater DNA duplex binding affinity ($R^2 = 0.82$). Quantification of relative quadruplex and duplex binding affinity constants puts some of these ligands among the most selective quadruplex DNA interactive agents reported to date.

Introduction

The pyrido[4,3,2-*kl*]acridine ring system exemplified by necatarone **1** has been elaborated in nature by the fungus *Lactarius necator*.[2] In previous papers in this series we have described a range of synthetic routes to, and biophysical and biological properties of, DNA-affinic tetracyclic derivatives of 7*H*-pyrido[4,3,2-*kl*]acridine **2**[3] generally substituted in the 2- and/or 3-position and pentacyclic 8*H*-quino[4,3,2-*kl*]acridines **3a** substituted in the 2- or 3-position including benzo annelation, as well as their 8-alkyl derivatives **3b**,**c** (Figure 1).[3–6] Compounds of series **2** and **3** are relatively weak bases; for example, the pK_a for the amino-substituted pentacycle **3d** is 6.18 and solutions of its methanesulfonic acid salt dissociate to precipitate the insoluble free base at physiological pH.[4] These compounds have only modest growth-inhibitory properties in the NCI60 human cell line screen[7] with mean GI_{50} [a] values usually in the range of 10–100 μM for tetracycles and 1–10 μM for the more inhibitory pentacycles; peripheral substituents have little effect on activity (mean GI_{50} for **3d** is 1.48 μM). Variants with the potential to be fully protonated at physiological pH have more potent growth-inhibitory activities, as would be predicted from a knowledge of the history of bioactive acridines.[8] For example, the 13-methylquinoacridine **4** (a modified 9-anilinoacridine) is more potent (mean GI_{50} of 0.32 μM) and the hexacyclic structure **5** is a further 5-fold more growth-inhibitory (mean GI_{50} of 0.06μM).[5] The indolizino[7,6,5-*kl*]acridinium chloride **6** (mean GI_{50} value of 0.09 μM) is a potent inhibitor of topo II and, like **4** and **5**, shows strong mechanistic comparisons in the NCI COMPARE analysis (Pearson correlation coefficients of >0.6)[7] with a range of DNA duplex binding topo II inhibitors.[4]

NCI60 assays (2-day drug exposure) give only limited information on mechanisms of drug action; for these DNA-affinic polycyclic systems more precise physicochemical measurements are required to determine which DNA polymorphic form is the "target". Thus, ^{1}H NMR, optical spectrometry, and molecular modeling studies have revealed that **6** makes an intercalative interaction with CpG sequences in duplex DNA.[9] A further structural type, exemplified by the quaternized diethylquino[4,3,2-*kl*]acridinium iodide **7**, originally synthesized by Polish chemists,[10] cannot undergo deprotonation (or further protonation) within the physiological pH range and has been shown by competition dialysis experiments and other methods to exhibit strong affinity for triplex DNA.[11] We have reported previously that examples of a new series of quaternized quino[4,3,2-*kl*]acridinium salts **8a**−**d** associate strongly with quadruplex DNA.[12,13]

Quadruplex DNA structures (G-quadruplexes) are formed within guanine-rich oligonucleotides and consist of stacks of planar G-tetrads stabilized by cations in or between the G-tetrad planes.[14] Recent reports suggest that the human genome may contain over 300 000 sequences potentially capable of forming quadruplexes, notwithstanding modulation by dynamic equilibrium between structural forms of DNA and the influence of chromatin structure and DNA binding proteins.[15] Notably, G-rich DNA, with the ability to form quadruplex structures, occurs at the telomere 3′ ends.[16] Telomeres protect chromosomal termini from exonucleases and ligases, thus preventing degrada-

* To whom correspondence should be addressed. Phone: +44 (0)115 951 3414. Fax: +44 (0)115 951 3412. E-mail: malcolm.stevens@nottingham.ac.uk.

[†] University of Nottingham.

[#] The Open University.

[‡] Georgia State University.

[§] Museum National d'Histoire Naturelle.

[a] Abbreviations: SPR, surface plasmon resonance; FRET, fluorescence resonance energy transfer; TRAP, telomere repeat amplification protocol; NCI60, National Cancer Institute 60 cell line in vitro screen; *Q*/*D*, quadruplex to duplex DNA binding affinity ratio; SI, selectivity index; IC_{50}, 50% inhibitory concentration; GI_{50}, 50% growth inhibitory concentration; ΔT_m, change in melting temperature; ST-DNA, salmon-testis DNA; m-AMSA, amsacrine.

10.1021/jm070587t CCC: $40.75
Published on Web 02/02/2008

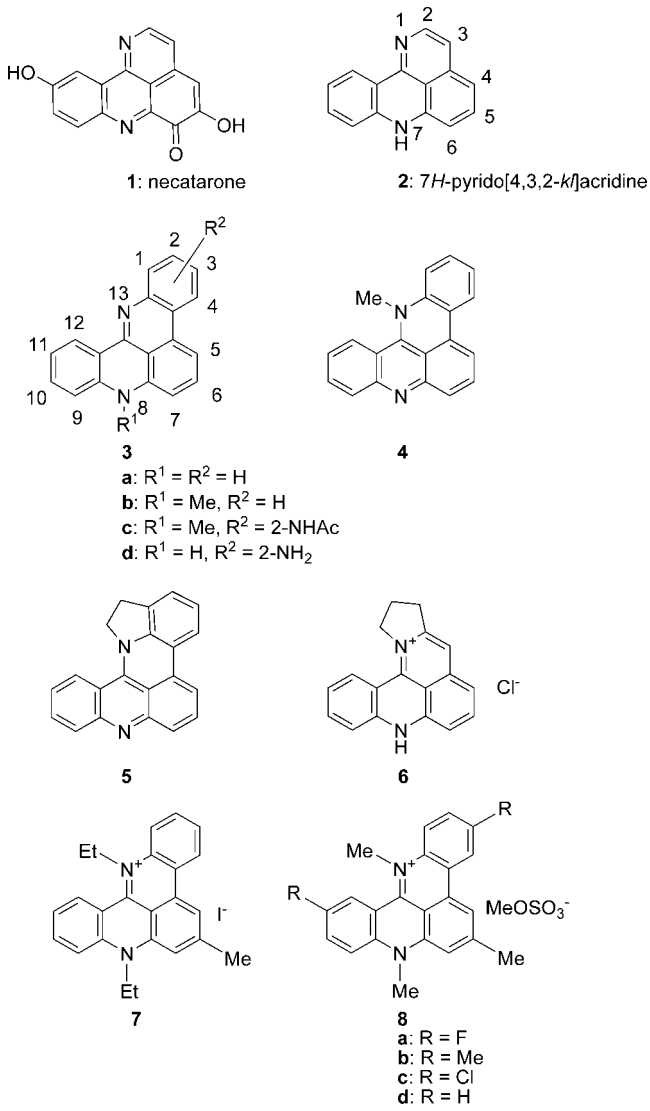

Figure 1. Structures of bioactive polycyclic acridines.

tion or end-fusion and maintaining stability.[17] Differing intramolecular G-quadruplex structures formed by the human telomeric repetitive DNA sequence $(TTAGGG)_n$ have been described depending on the conditions and technique employed.[18–20] Potassium-stabilized G-quadruplex structures formed by the telomere substrate in vitro inhibit telomere maintenance by the enzyme telomerase.[21]

Elevated telomerase activity has been implicated in ~85% of cancers, reflecting their immortal nature,[22] and its inhibition represents a strategy for the development of selective anticancer drugs.[23,24] G-quadruplex-interactive inhibitors of telomerase may offer a less challenging developmental pathway to the clinic than antisense agents targeted directly against components of the telomerase ribonucleoprotein complex.[25] The discovery of proteins with roles specific to G-quadruplex DNA is strongly indicative of an in vivo role for these structures and confounds the scepticism of critics of the potential relevance of this novel molecular target in anticancer drug design. For example, proteins that bind to and promote the formation of G-quadruplexes in yeast telomeres,[26] G-quadruplex-specific nucleases,[27] and helicases that can resolve G-quadruplex structures[28] have been identified. Furthermore, a specific antibody can locate the presence of a G-quadruplex in *Stylonychia* telomeres in vivo.[29] Putative quadruplex sequences also occur in many G-rich gene promoter regions,[30] for example, the c-*myc* oncogene, for which G-quadruplex formation appears to regulate gene expression.[31]

Different structures have been identified with high affinity and selectivity for the human quadruplex telomeric sequence. These include anthraquinones, porphyrins, ethidium bromide derivatives, fluorenones, heteroaromatic polycyclic systems, quinolines, trisubstituted acridines, and the natural product telomestatin (for reviews, see refs 25 and 32). The quino[4,3,2-*kl*]acridinium methosulfate **8a** (RHPS4) stabilizes quadruplex DNA, provokes telomeric disruption,[33] and is a potent inhibitor in the TRAP assay ($IC_{50} = 0.33\ \mu M$), a property shared with salt **8b** although the broader pharmacological properties of **8a** and **8b** diverge.[12] Compound **8a** has been selected as a lead compound for in vivo evaluation from this novel class of "telomere-targeted agents" on the basis of its synthetic accessibility,[1] water-solubility, stability to a panel of cytochrome P450s, and robust druglike properties.[34]

In past work we have reported the synthesis of a range of structurally diverse quino[4,3,2-*kl*]acridinium salts **8a**−**d**, and **9a**−**z** (Figure 2), and in this paper we have collated their growth-inhibitory activities against tumor cell lines in vitro (NCI60 assays) and their telomerase-inhibitory activities as inferred from the TRAP assay and studied the ability of selected compounds to bind to different DNA isoforms by physicochemical methods. In particular we were interested in identifying new agents with abilities to potently stabilize quadruplex DNA with the intention of selecting an agent(s) as a potential backup(s) to **8a**.

Survey of Published Synthetic Routes to Quino[4,3,2-*kl*]acridinium Salts. In considering alternatives to **8a**, we have exploited our experiences in thermal, radical, and palladium(0)-mediated chemistry to synthesize compounds with uncharged side chains, especially at the 2-, 3-, 6- and 10-positions, where opportunities for additional binding in the quadruplex grooves have been identified.[34,35] Briefly, the following methods have been used (see Experimental Section for references to specific syntheses): compounds **8a**−**d** were prepared by the multistep "one-pot" Ozczapowicz synthesis[10] starting from 6-substituted 1,2-dimethylquinolinium methosulfates **10** (Scheme 1). The bromophenyliminoacridine **11** was subjected to radical cyclization to yield **3b**, which was further processed by methylation with methyl iodide to generate **9a**. Syntheses of the 2-amino-substituted dimethylquino[4,3,2-*kl*]acridinium iodides **9b**−**m** were approached from the 9-(6-nitrobenzotriazol-1-yl)acridine **12**, which was thermolyzed in triglyme at 216 °C to give the nitro-substituted pentacycle **13**. This was successively methylated at N-8 and then reduced to give the amine **14**, which was further methylated to give **9b**. Monomethylation or dimethylation at the exocyclic amino group of **14** followed by quaternisation at N-13 afforded derivatives **9c**,**d**. Acetylation of the exocyclic amino group of **14** gave the *N*-acetylaminoquinoacridine **3c**, which could be methylated to yield the 2-acetylaminoquinoacridine **9e**. Alternatively, reactions between **14** and a range of acylating and sulfating agents followed by methylation at N-13 afforded derivatives **9f**−**m**. 9-(5-Chlorobenzotriazol-1-yl)acridine **15** was a convenient starting point to the *N*-acetylaminoquinoacridinium iodide substituted in the 3-position, **9n**: thermolysis of **15** in triglyme gave the 3-chloroquinoacridine **16**, which was methylated at N-8, and the chloro group was replaced by benzylamine in a Pd(0)-mediated reaction to yield **17**. Reductive debenzylation of **17**, followed by acetylation of the amino group and meth-

Scheme 1. Outline of Synthetic Routes to Quaternary Quinoacridinium Salts **8a**−**d** and **9a**−**z**

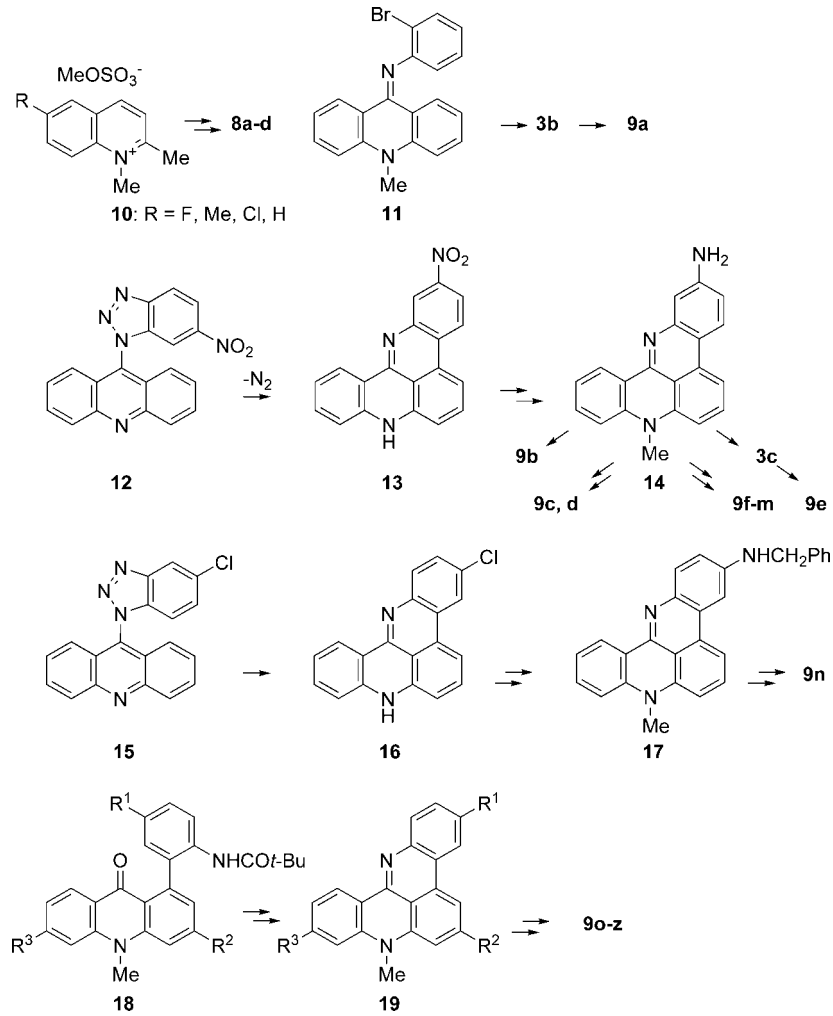

ylation at N-13, gave **9n**. Syntheses of quinoacridinium salts substituted in the 3- and/or 6- and/or 10-position(s), **9o**−**z**, were more complex and required the construction of protected substituted *N*-methylacridones **18**, which could be cyclized to pentacycles **19** with appropriate $R^1R^2R^3$ groups (e.g., Cl, Br, CF_3SO_2O) amenable to efficient orthogonal substitution in Pd(0)-mediated Suzuki−Miyaura or Heck coupling reactions, followed by methylation at N-13. For example, Heck replacement of the 3-chloro group of **19** (R^1 = Cl, $R^2 = R^3$ = H) with 4-acryloylmorpholine in the presence of $Pd_2(dba)_3$ catalyst and ligand P(*t*-Bu) afforded **19** (R^1 = CH=CH-$CON(CH_2CH_2)_2O$, $R^2 = R^3$ = H) in 92% yield, which could be methylated with methyl iodide in a sealed tube at 100 °C to produce the iodide salt **9w** (Scheme 1).

Results

In Vitro Activities of Quinoacridinium Salts 7, 8a−d, and 9a−z against Human Cell Lines (NCI60) and COMPARE Analysis. Overall, there was a 300-fold range in mean growth-inhibitory potencies in the NCI60 cell panel (Table 1).[7] Incorporation of extended neutral substituents into the 3-, 6-, or 10-position (compounds **9r**−**z**) was not reflected in enhanced growth-inhibitory activity, and the least potent compound was the 6,10-disubstituted quaternary salt **9t** with a mean GI_{50} value of >100 μM. The most potent salts were **8b**, **9c**, and **9d** (mean GI_{50} values of <0.5 μM).

The COMPARE algorithm is a reliable method for detecting which chemical structures in the NCI database might share (or not share) a common pharmacological mechanism.[36] In previously published work we have shown that the methosulfate salts **8a**,**b**, which are closely related structurally, display different patterns of activity in the COMPARE analysis; the more weakly inhibitory difluoroquinoacridinium salt **8a** (mean GI_{50} of 13.18 μM) shows no Pearson correlation coefficient (PCC) values of >0.6 to clinically evaluated agents, whereas the potent 3,11-dimethyl analogue **8b** shows mechanistic similarities to duplex DNA-interactive agents actinomycin D, bactobolin, bisantrene, and chromomycin (PCC values of >0.65).[12] (Note: a PCC value of >0.65 strongly suggests a significant mechanistic link between different agents.)[36] This distinction was corroborated in the present study where **8a** was shown to increase T_m of ST-DNA by 10.8 °C, compared to 16.6 °C for **8b** (data not shown), consistent with the emerging picture of compound **8b** being a more potent duplex DNA ligand. Similarly **9d** gave PCC values of >0.65 with the clinically used duplex DNA-interactive agents bisantrene hydrochloride, actinomycin D, rubidazone, adriamycin, and daunomycin. In a more detailed analysis (see Supporting Information, Table S1) application of the amines **9c**,**d** or the 6-methoxy-10-chlorodimethylquinoacridinium salt **9p** as "seeds" in the COMPARE analysis gave consistently high PCC values (>0.75) within the three-compound set but less so with the acetamide **9e** (PCC = 0.41–0.64). To show the utility of the method, compound **3c**, which is unmethylated at N-13, was included in the analysis and shows no mechanistic similarities to the other four compounds (PCC = 0.04–0.41). Clearly, in

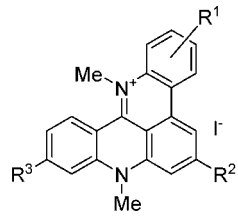

Compd.	R^1	R^2	R^3
9a	H	H	H
9b	2-NH_2	H	H
9c	2-NHMe	H	H
9d	2-NMe_2	H	H
9e	2-NHAc	H	H
9f	2-$NHCOCF_3$	H	H
9g	2-NHCO*n*-Bu	H	H
9h	2-NHCO*t*-Bu	H	H
9i	2-$NHCO(CH_2)_4CO_2Me$	H	H
9j	2-$NHCO(CH_2)_{10}Me$	H	H
9k	2-$NHCO_2Et$	H	H
9l	2-NHCOPh	H	H
9m	2-$N(Me)SO_2C_6H_4F$-*p*	H	H
9n	3-NHAc	H	H
9o	3-Cl	OMe	H
9p	H	OMe	Cl
9q	3-Cl	H	H
9r	H	OMe	$CH{=}CHCON(CH_2CH_2)_2O$
9s	H	OMe	$CH{=}CHCO_2Me$
9t	H	OMe	$CH{=}CHCON(CH_2CH_2)_2O$
9u	H	$(CH_2)_3OAc$	$(CH_2)_3OAc$
9v	3-Cl	$CH{=}CHCON(CH_2CH_2)_2O$	H
9w	3-$CH{=}CHCON(CH_2CH_2)_2O$	H	H
9x	3-$CH{=}CHCON(CH_2CH_2)_2O$	OMe	H
9y	3-$CH{=}CHCON(CH_2CH_2)_2O$	$(CH_2)_3OAc$	H
9z	3-$(CH_2)_3OAc$	$(CH_2)_3OAc$	H

Figure 2. Structures of 8,13-dimethylquinoacridinium iodides.

these structures, possession of a quaternary structure is a major determinant of biological activity.

TRAP-Inhibitory Activity of Quaternized Quinoacridinium Salts. A selection of compounds were evaluated as telomerase inhibitors in the TRAP assay (Table 1). Detection of false positives due to inhibition of Taq DNA polymerase (in the PCR amplification step) was accomplished by prescreening all the compounds for Taq polymerase inhibition, which typically occurred at concentrations of 10 μM or above, and TRAP assays were only conducted at non-Taq polymerase-inhibitory concentrations (data not shown).[37] The least potent of the quinoacridinium salts tested in the TRAP assay were **7** and **9a**,**b** with $^{TRAP}IC_{50}$ values in the 1.5–2 μM range (Table 1). Other compounds were generally 5-fold more potent ($^{TRAP}IC_{50}$ = 0.21–0.74 μM). On the reasonable assumption at this point that growth-inhibitory potency as described above (48 h of drug exposure) might be linked with untoward toxicological sequelae attributable to duplex DNA binding, whereas interference with telomere maintenance would be attributed to quadruplex binding, a high selectivity index (SI = (mean GI_{50})/$^{TRAP}IC_{50}$) was considered desirable. The least selective compounds were **7** (SI = 0.6), **8b** (SI = 1.6), **8d** (SI = 1.7), and **9b** (SI = 1.9), whereas those with the highest SIs were **8a** (SI = 40) and, notably, **9n** (SI = 195) and **9w** (SI = 183) (Table 1). A

Table 1. In Vitro Growth Inhibitory Properties (Mean GI_{50} Values) and TRAP Inhibitory Activity ($^{TRAP}IC_{50}$) of Quinoacridinium Salts

compd	mean GI_{50}[a] (μM)	$^{TRAP}IC_{50}$[b] (μM)	selectivity index (SI)[c]
7	1.10	2.00	0.6
8a	13.18	0.33	40.0
8b	0.41	0.25	1.6
8c	4.71		
8d	1.29	0.74	1.7
9a	7.58	1.55	4.8
9b	3.55	1.86	1.9
9c	0.46		
9d	0.28		
9e	12.00	0.38	32.0
9f	2.20	0.31	7.0
9g	1.00		
9h	3.30	0.23	14.0
9i	6.02	0.21	27.0
9j	0.54		
9k	0.66		
9l	6.61		
9m	10.00	0.73	14.0
9n	81.30	0.41	195.0
9o	0.74	0.28	2.6
9p	0.75		
9q	3.16	0.26	12.0
9r	43.60		
9s	4.57		
9t	>100		
9u	3.31		
9v	12.30		
9w	67.60	0.37	183.0
9x	9.33		
9y	27.50		
9z	3.80		

[a] NCI60 cell panel (ref 7). [b] TRAP assay (for method see ref 37); results are the mean of at least three determinations. [c] Mean $GI_{50}/^{TRAP}IC_{50}$.

representative TRAP assay gel and its quantification are shown for compound **9i** in Supporting Information (Figure S1).

Interaction of Quaternized Quinoacridinium Salts with Quadruplex and Duplex DNA. (i) Fluorescence and UV Titrations. Interaction between a ligand and a nucleic acid leads to optical changes that can be measured during titration. Polycyclic acridinium salts show fluorescence quenching when binding to duplex and quadruplex DNA and a bathochromic shift in UV absorbance when binding to duplex DNA.

Fluorescence titration experiments were performed with the G-quadruplex forming human telomeric sequence d[AG_3-$(TTAGGG)_3$] to yield the equilibrium binding constants for a series of polycyclic acridines (Table 2). Representative binding profiles for weak **9a** ($K = 9.1 \times 10^4$) and strong **9h** ($K = 1.1 \times 10^6$) G-quadruplex binding ligands are shown in Figure 3. Fluorescence titration against duplex genomic DNA from salmon testis (ST-DNA), which consists of approximately 58.8% AT and 41.2% GC, showed that binding to this sequence varied over an 8-fold range between the strongest **8b** ($K = 2.4 \times 10^5$) and weakest **9w** ($K = 3.1 \times 10^4$) (binding curves shown in Supporting Information, Figure S2). The data in Table 2 confirm that quaternized polycyclic acridines interact with quadruplex DNA more avidly than with duplex. The ratio of the binding constants for quadruplex and duplex DNA (Q/D) by this technique reveals that **9i** and **9w** exhibit the highest selectivity for quadruplex DNA ($Q/D > 10$); salts **9a** and **9z** were the least discriminatory ($Q/D < 2$).

Evaluation of selected analogues **8a** and **8b** by the fluorescence titration technique shows weaker binding affinity of **8a** compared to **8b** for the ST-DNA duplex ($K = 5.6 \times 10^4$ compared to 2.4×10^5). For a detailed comparison of duplex DNA-binding behavior between **8a** and **8b**, these analogues were tested for duplex DNA binding affinity by UV titration

Table 2. Equilibrium Binding Constants (K) of Quaternary Polycyclic Acridinium Salts to Quadruplex and Duplex DNA Determined by Fluorescence Titrations and Surface Plasmon Resonance.

	fluorescence titration[a]			surface plasmon resonance[b]		
	$K \times 10^5$ M^{-1}			$K \times 10^5$ M^{-1}		
compd	quadruplex (Q) DNA[c]	duplex (D) DNA[d]	Q/D	quadruplex (Q) DNA[c]	duplex (D) DNA[e]	Q/D
8a	2.70	0.56	4.8	110.0	3.4	32.3
8b		2.40		74.0	5.4	13.7
9a	0.91	0.71	1.3			
9e	3.70	0.63	5.9	240.0	3.8	63.0
9f	6.00	0.70	8.6	130.0	3.8	34.2
9h	11.00	1.20	9.2			
9i	10.00	0.68	14.7			
9m	1.90	0.83	2.3	48.0	17.0	2.8
9n	3.10	0.53	5.8	250.0	4.4	57.0
9o	6.40	2.20	2.9			
9q	6.70	1.10	6.0			
9w	3.20	0.31	10.3	71.0	25.0	2.8
9z	1.60	0.94	1.7	2.4	1.7	1.4

[a] Buffer solution: 185 mM NaCl, 6 mM Na_2HPO_4, 2 mM NaH_2PO_4, 0.1 mM EDTA, pH 7.0. [b] Buffer solution: 10 mM HEPES buffer (pH 7.4) containing 200 mM KCl, 3 mM EDTA, and 0.005% surfactant P20. [c] Human telomeric sequence d[$AG_3(TTAGGG)_3$]. [d] ST-DNA. [e] d[$(CG)_8$] alternating GC eight base pair hairpin sequence.

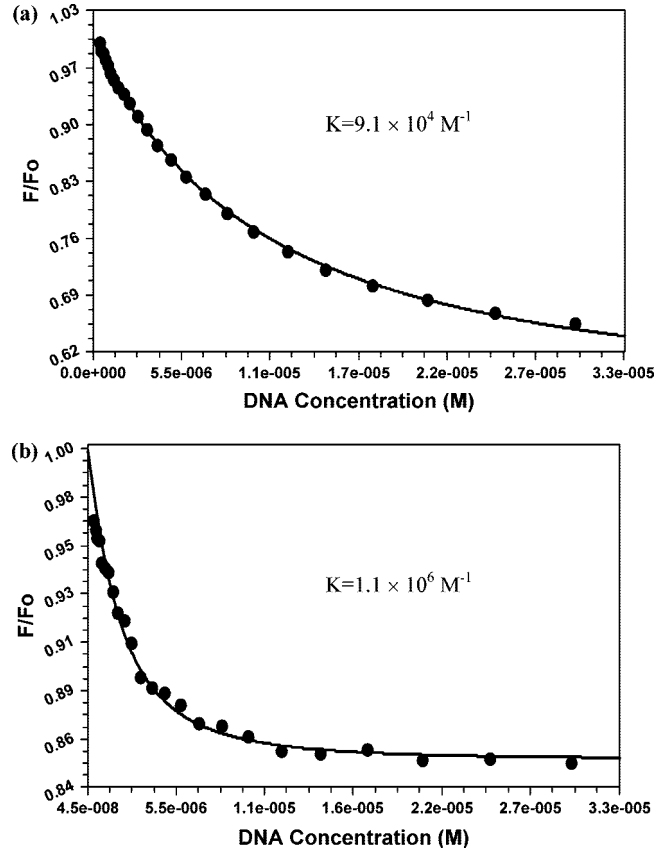

Figure 3. Representation of (a) weak **9a** and (b) strong **9h** quadruplex binding ligands: (●) raw data points obtained by fluorescence titration; (−) model generated fit (see text). K values are equilibrium binding constants. The quadruplex DNA sequence used was the human telomeric sequence d[$AG_3(TTAGGG)_3$].

against a number of duplex DNA sequences: ST-DNA (see above), nonalternating poly[dA]·poly[dT] and poly[dG]·poly[dC], and alternating poly[dA-dT]$_2$ and poly[dG-dC]$_2$. Equilibrium binding constants (K) of both analogues to each DNA were calculated using the model of Missailidis.[38] Both compounds demonstrate capability for binding to duplex DNA but possess

Table 3. Duplex DNA Binding Affinity and Stabilization by Compounds **8a** and **8b** Determined by UV Titration

DNA sequence	K^a	
	8a	**8b**
ST-DNA	2.0×10^5	8.0×10^6 (s), 2.6×10^4 (w)
poly[dA]·poly[dT]	8.0×10^4	4.0×10^6 (s), 8.0×10^5 (w)
poly[dA-dT]$_2$	6.0×10^5	4.0×10^5 (s), 1.0×10^4 (w)
poly[dG]·poly[dC]	1.0×10^6	1.0×10^6 (s), 5.0×10^4 (w)
poly[dG-dC]$_2$	6.0×10^6	1.2×10^6

[a] Equilibrium constant determined by UV titration for compounds with DNA sequences. "s" in parentheses indicates the stronger binding mode, and "w" in parentheses indicates the weaker.

different binding profiles; **8a** exhibits one single strong binding mode (Table 3) especially to G-C sequences, whereas **8b** exhibits a stronger (K_s) and a weaker (K_w) mode to most sequences. Example binding curves are included in Supporting Information (Figure S3). The presence of two binding modes has been reported before for unquaternized acridine derivatives of different types binding to duplex DNA.[39] By UV titration, compound **8a** has 40-fold weaker affinity for ST-DNA compared to **8b** ($K = 2.0 \times 10^5$ and $K_s = 8.0 \times 10^6$, respectively), corroborating the findings with the fluorescence titration technique, albeit suggesting a greater differential between the two ligands than with UV. (Note: the overall K values determined by fluorescence titrations are lower than by UV; this is attributable to the higher ionic strength of the buffer in fluorescence experiments, which is known to reduce the binding of positively charged ligands to the negatively charged DNA.)[40]

(ii) Surface Plasmon Resonance (SPR). SPR is a suitable technique for quantitative comparison of binding affinities of DNA-interactive agents.[41] Binding of drug to DNA immobilized on a sensor chip surface causes a change in the refractive index at the surface and hence to the reflected light angle at which SPR is observed; the change in SPR response is directly related to the concentration of molecules at the surface. The SPR method used here is only applicable to the study of short, defined oligonucleotide sequences, and so no equivalent of the UV/fluorescence study of binding to ST-DNA was possible. SPR was used to analyze the binding of polycyclic salts to an alternating GC eight base pair hairpin (duplex) sequence (Table 2). By the SPR method the quinoacridinium salt substituted with an acryloylmorpholine substituent at the 3-position, **9w**, had the highest binding affinity to duplex DNA but not in the fluorescence titration experiments. Possible reasons for this discrepancy are the different duplex sequences used in the different methods. Also, sodium was the cation present in the fluorescence titrations whereas it was potassium for SPR experiments. This would be expected to influence quadruplex stability.

SPR results (Table 2) confirm that quaternary salts bind more strongly to quadruplex DNA (human telomeric sequence) than duplex (alternating GC eight base pair hairpin). The isomeric 2- and 3-acetylaminoquinoacridinium salts **9e** and **9n** were most selective to stabilize the quadruplex structure according to the SPR experiments. In general, agreement between the fluorescence and SPR methods was good for compounds where corresponding G-quadruplex binding data are available for comparison; the correlation is shown in Supporting Information (Figure S4).

SPR has the advantage of providing kinetic as well as equilibrium characterization of interactions between nucleic acids and small molecules.[42] Representative sensorgrams for binding of **9e** to both duplex and quadruplex sequences are shown in Figure 4a, and a direct binding plot is shown in Figure 4b. The sensorgrams show interesting kinetics: whereas the duplex has very fast on/off kinetics (Figure 4ai), the quadruplex sequence (Figure 4aii) shows slow dissociation in the lower half of the sensorgram, representing a strong binding mode, and fast dissociation in the upper half, suggestive of a weaker binding event. This is in accord with NMR studies of the interaction of **8a** with a parallel stranded quadruplex DNA, which revealed that the molecule stacks at two nonequivalent sites, one above and one below the G3 core of the quadruplex.[13] The marked selectivity of **9e** and **9n** for quadruplex DNA in SPR experiments (~60-fold greater affinity for the G-quadruplex sequence compared to the duplex) compares favorably to other G-quadruplex ligands reported in the literature such as BRACO-19 (40-fold selectivity)[43] and BOQ1 (~10-fold selectivity),[44]

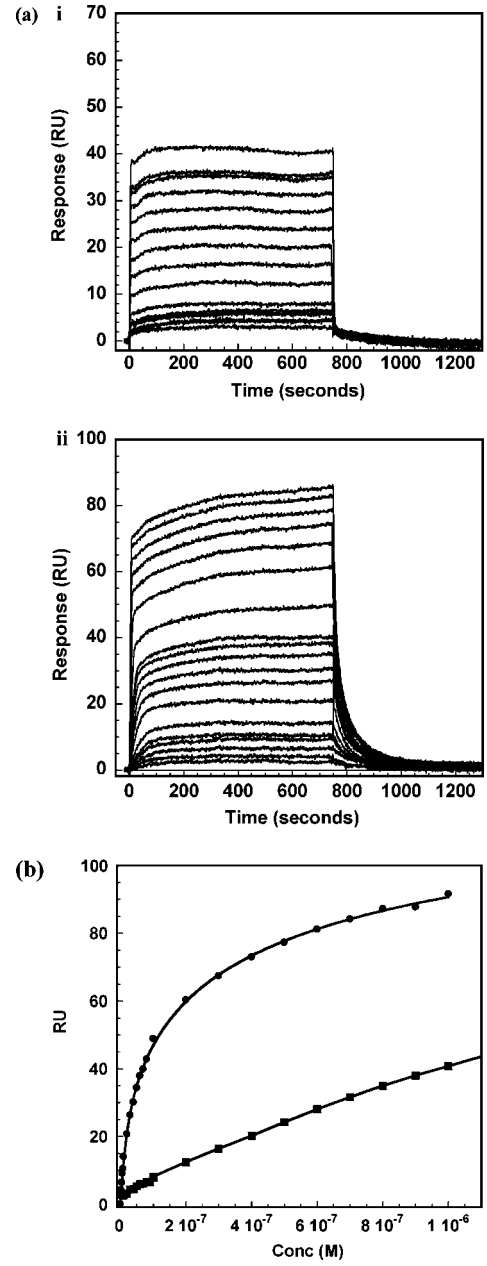

Figure 4. SPR experiments with **9e**. (a) Representative sensorgrams for **9e** binding to (i) duplex (CG eight base pair hairpin d[(CG)$_8$]) and (ii) quadruplex (human telomeric d[AG$_3$(T$_2$AG$_3$)$_3$]) DNA sequences. The lines are best fits to the steady-state RU (response units) values, which are directly proportional to the amount of bound compound. (b) Direct binding plot for **9e** of RU versus concentration of unbound **9e**: (●) quadruplex; (■) duplex (for sequences, see part a). The lines are obtained by nonlinear least-squares fits of the data.

Table 4. Stabilization of the F21T DNA Quadruplex Sequence[a] to Thermal Denaturation by Quaternary Polycyclic Acridinium Salts[b] (FRET Analysis)

compd	ΔT_m (°C)[c]	compd	ΔT_m (°C)[c]
m-AMSA	0.0	**9d**	3.8
7	0.0	**9e**	10.0
8a	8.0	**9o**	9.0
8b	7.0	**9q**	5.0
8d	2.0	**9w**	4.5
9a	2.8	**9z**	0.5

[a] d[$G_3(T_2AG_3)_3$] modified with the covalent attachment of fluorescein at the 5′ end and tetramethylrhodamine (tamra) at the 3′ end (F21T). [b] At 1 μM compound. [c] Ligand-induced changes in melting temperature.

making **9e** and **9n** among the most selective G-quadruplex interactive agents to be identified by this method.

(iii) Fluorescence Resonance Energy Transfer (FRET). F21T is a FRET system characterized by Mergny and co-workers[45,46] as consisting of the quadruplex-forming oligonucleotide d[$G_3(T_2AG_3)_3$] synthesized with the donor molecule fluorescein at the 5′ end and the acceptor molecule tetramethylrhodamine (tamra) at the 3′ end. In the folded quadruplex state, the 5′ and 3′ termini of the oligonucleotide are in proximity to each other and a strong FRET signal is observed. Upon thermal denaturation (melting), the distance between the fluorescein and tamra molecules increases, and therefore, FRET decreases. This process can be followed by fluorimetry to determine the melting temperature of the oligonucleotide (T_m) and any ligand-induced change (ΔT_m). The test is performed in a lithium chloride buffer. The sodium concentration is kept low (10 mM) in order to decrease quadruplex stability while keeping the ionic strength relatively high with lithium, which is less favorable for quadruplex formation than sodium or potassium, and so any stabilization caused by an interacting ligand is easier to detect.[45] T_m was calculated as the temperature at which the fluorescence intensity of the melting oligonucleotide (normalized between 0 and 1) equaled 0.5.

FRET results with the quadruplex probe F21T obtained for a series of salts are shown (Table 4). With the exception of the control agent *m*-AMSA and compound **7**, all the derivatives stabilized F21T to melting temperatures, with the 2-acetamino-substituted pentacycle **9e** conferring the greatest ΔT_m on the quadruplex (ΔT_m = 10.0 °C) and **9z** (ΔT_m = 0.5 °C) the least. Good correlation was observed between the FRET ΔT_m data and quadruplex binding affinity constants obtained by SPR (see Supporting Information, Figure S4). The melting profiles of F21T in the absence and presence of *m*-AMSA, **8a**, and **9e** are included in Supporting Information (Figure S5).

(iv) Competition Dialysis. We have used this technique previously, wherein a number of dialysis units, each containing a different DNA sequence, are included within a single system to determine ligand selectivity for particular DNA sequences/polymorphs,[47] to show that salts **8a** and **8b** differ in their relative affinities for different DNA structures:[12] the propensity of **8a** to bind selectively to higher-order structures (triplex and quadruplex) as opposed to the more promiscuous binding of **8b** to single- and double-stranded DNA, as well as triplex and quadruplex sequences, is entirely consistent with the biological and biophysical data presented above.

In the present competition dialysis study two further members of the series, **9b** and **9e**, were compared with reference compound **6**. The acridinium chloride **6** showed little discrimination between the range of different DNA structures (Figure 5a). Indeed, its biological activity (potent growth-inhibitory properties and topo II inhibitory activity[4]) is probably a consequence of its avid binding to duplex DNA. As we have

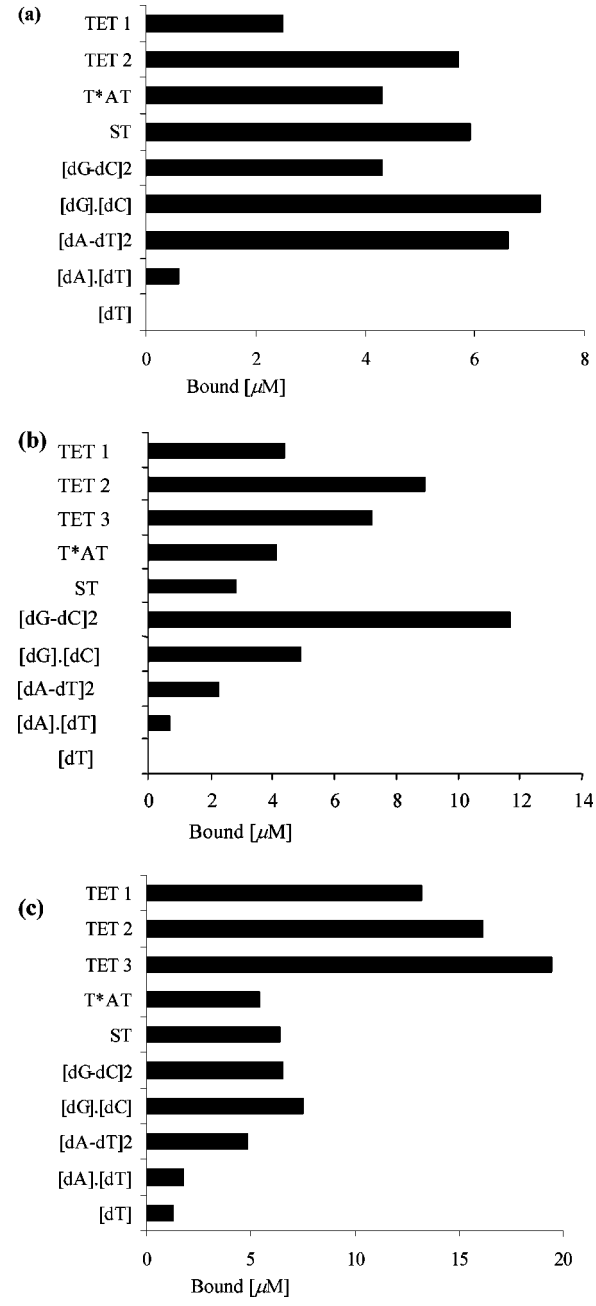

Figure 5. Relative affinities of the polycyclic acridine derivatives for different DNA polymorphs determined by competition dialysis: (a) **6**; (b) **9b**; (c) **9e**; TET 1 (quadruplex), d[$T_2G_{20}T_2$]$_4$; TET 2 (quadruplex), d[$AG_3(T_2AG_3)_3$] (human telomeric sequence); TET 3 (quadruplex), d[T_4G_4]$_4$; T*AT (triplex), poly[dT]*poly[dA]·poly[dT]; ST (duplex), salmon testis DNA; [dG-dC]$_2$ (duplex), poly[dG-dC]·poly[dG-dC]; [dG]·[dC] (duplex), poly[dG]·poly[dC]; [dA-dT]$_2$ (duplex), poly[dA-dT]·poly[dA-dT]; [dA]·[dT] (duplex), poly[dA]·poly[dT]; [dT] (single-stranded), poly[dT]. Studies were performed at 2 μM drug compound.

shown previously, the quaternary quinoacridinium salt **8a** binds preferentially to triplex and quadruplex structures,[12] generating a biological profile consistent with telomere-targeted activity. The 2-aminoquinoacridinium salt **9b** bound with particular affinity to the duplex poly[dG-dC]$_2$ polymorph, less so to the quadruplex sequences (Figure 5b) and consistent with the COMPARE behavior of the related amines **9c** and **9d**, which links their biological activity to topoisomerase II inhibition. In contrast, the *N*-acetyl derivative **9e**, which had shown promising G-quadruplex affinity in earlier experiments (FRET and SPR),

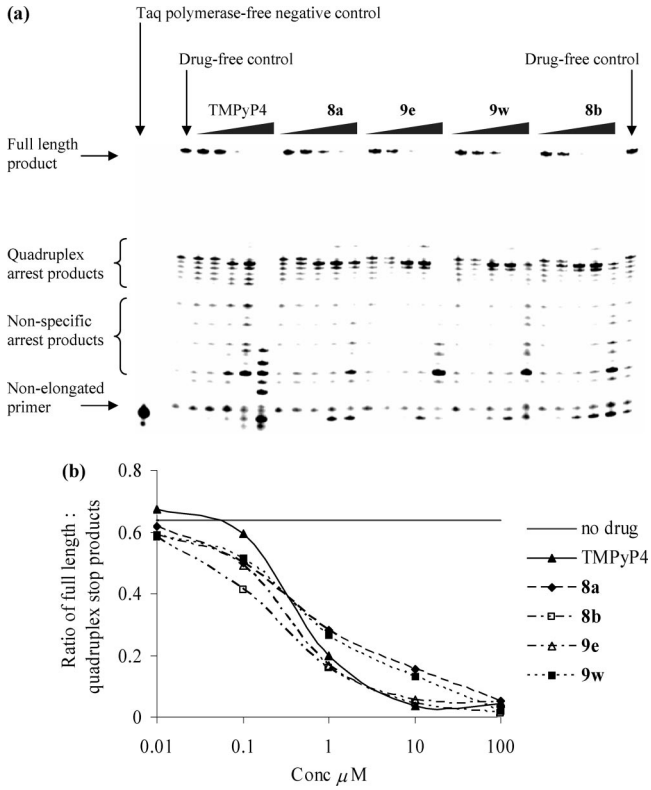

Figure 6. G-quadruplex stabilization in the human *c-myc* Pu27 DNA sequence (of the NHE III region of the P1 promoter) in the presence of TMPyP4, **8a**, **8b**, **9e**, and **9w** (Taq polymerase arrest assay). (a) Denaturing gel showing products of Taq polymerase elongation of primer in the presence of ligand (0.01, 0.1, 1, 10, 100 μM L → R indicated by thickening line). (b) Quantification of gel shown in (a). The intensities of the bands on the gel representing the proposed full-length product (77-mer) and G-quadruplex arrest products (intermediate length) were determined using ImageQuant software, and the ratio was plotted against drug concentration.

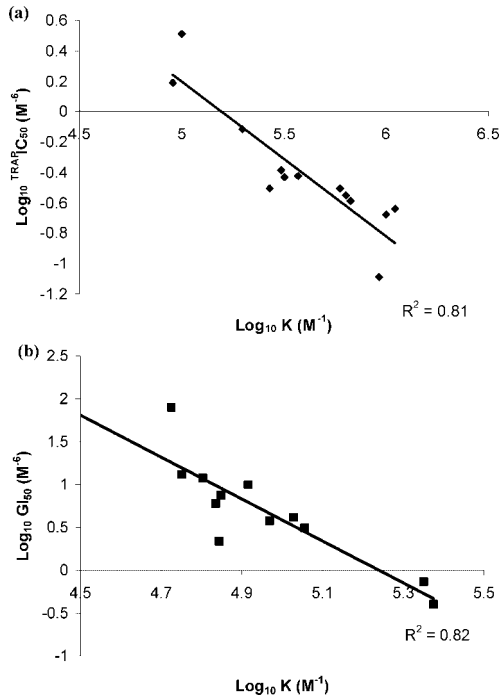

Figure 7. Correlations between biophysical and biological properties of polycyclic acridines: (a) TRAP inhibition versus quadruplex binding affinities; (b) growth inhibition versus duplex binding affinities; (■) experimental data; (−) linear fits. Affinity constants (K) were obtained from fluorescence titration experiments (Table 2). Mean GI_{50} data were obtained from 2-day exposure in the NCI60 cell line panel (Table 1). $^{TRAP}IC_{50}$ data were from the TRAP assay (Table 1).

also exhibited the greatest selectivity for quadruplex DNA polymorphs by this technique (Figure 5c).

(v) Taq Polymerase Arrest Assay. G-quadruplex formation and stabilization in DNA sequences can be assessed by a Taq polymerase arrest assay in which a quadruplex-forming sequence of interest is incorporated into a cassette sequence that acts as a template for elongation of a radiolabeled primer by DNA polymerase. Formation of G-quadruplex structures impairs full-length sequence extension by the polymerase, a phenomenon visualized by electrophoresis and phosphorimaging of reaction products. Besides the telomeres, there are also other DNA targets that might contribute to the biological activity of these compounds. The promoter sequences of certain genes, *c-myc* and *bcl-2* for example, are thought to be capable of G-quadruplex formation, with implications for the modulation of gene expression.[31] The ability of polycyclic acridinium compounds to modulate one such sequence, the purine-rich 27-mer (Pu27) of the nuclease hypersensitivity element (NHE) III_1 of the P1 promoter of the *c-myc* oncogene, was examined in this assay.[31] Compounds **8a**, **8b**, **9e**, and **9w** were elected for study on the basis of screening of their pharmaceutical properties;[34] the reference compound TMPyP4 was also included.[31] Results are shown in Figure 6a. All the compounds induced impediments to the elongation of primer by DNA polymerase, with a dose-dependent decrease in full-length products relative to intermediate length products, consistent with stabilized G-quadruplex structures acting as a barrier to complete elongation of the primer sequence by the polymerase. All the compounds caused a 50% decrease in full length product relative to G-quadruplex arrest products (IC_{50}) at concentrations less than 1 μM (Figure 6b), although IC_{50} values obtained will depend on the template concentration used. A template incorporating the G-quadruplex-forming *Tetrahymena* telomeric sequence $(TTGGGG)_4$ was also employed, with similar results, shown in Supporting Information (Figure S6). These assays served to confirm the G-quadruplex stabilizing activities of quaternary quinoacridinium salts and suggest that the compounds might have G-quadruplex targets beyond those located in the human telomere.

DNA Quadruplex Binding Affinity Correlates with TRAP Inhibition. A plot of telomerase inhibitory potency inferred from $^{TRAP}IC_{50}$ values against quadruplex DNA binding affinity data from fluorescence titration experiments for all the members of the series for which such data are available shows a strong positive correlation ($R^2 = 0.81$) (Figure 7a), supporting the hypothesis, also observed in other series of (unrelated) structures,[43,45,48–51] that G-quadruplex stabilization is the underlying mechanism for this inhibition and that G-quadruplex structures in the telomeric sequence are stabilized by these compounds. G-quadruplex structures have been proposed to prevent access to, and elongation of, the telomere substrate by the telomerase catalytic subunit.[21,25] No significant relationship can be seen between duplex DNA binding affinity and TRAP inhibition (shown in Supporting Information, Figure S7a).

DNA Duplex Binding Affinity Correlates with Growth Inhibitory Potency. There is a significant relationship between duplex DNA binding affinity as determined from fluorescence titration experiments and growth-inhibitory potency as determined by mean GI_{50} values in the NCI60 panel ($R^2 = 0.82$) (48-h exposure) (Figure 7b) but not between duplex DNA

binding and TRAP inhibitory potency (shown in Supporting Information, Figure S7b).

Discussion

Our studies on the synthesis and biological evaluation of a range of quino[4,3,2-*kl*]acridines started 15 years ago and have led to the identification of the quaternary salts **8a**−**d** as worthy of interest.[12] The selection of **8a** as a clinical candidate was predicated on its robust pharmaceutical properties,[34] combined with relatively low growth-inhibitory activity (e.g., no topoisomerase II inhibitory activity) and high potency in the TRAP assay ($^{TRAP}IC_{50} = 0.33\ \mu M$) represented by the high selectivity index (SI = 40). Since the discovery that the "capping" status of telomeres is a critical determinant of cell fate,[17] it is generally acknowledged that this class of agent may exert profound *acute* effects by disruption of telomeric integrity, consequent on their stabilizing the telomeric single-stranded DNA in the form of a G-quadruplex[25,33,49b,52] rather than by overt telomerase inhibition per se.[51,53] Consistent with the paradigm of telomere disruption, compound **8a** provokes the initial dissociation of the capping protein Pot-1 from the telomere, which then triggers recruitment of the DNA damage recognition machinery.[54] Significantly, **8a** exhibits potent and rapid in vivo activity against a panel of human tumor xenografts at well-tolerated doses.[54]

Fifteen compounds were evaluated for activity as potential telomerase inhibitors using the TRAP assay (Table 1). Despite the structural variations represented, potencies ($^{TRAP}IC_{50}$ values) vary only over a 10-fold range (0.21–2.0 μM). Two additional compounds **9n** and **9w**, previously unexplored in detail, also have very favorable SI values (195 and 183, respectively, Table 1), reflecting their low growth-inhibitory activities in the NCI60 screen coupled to high potency in the TRAP assay (Table 1).

In the evaluation of the wide range of quaternary salts reported here, it became important to attempt the difficult task of interpreting their biological properties in the light of their differential abilities to bind to different DNA isoforms; in particular, agents with selective abilities to stabilize quadruplex DNA relative to duplex DNA were sought. A range of physicochemical analytical methods (UV spectroscopy, fluorescence quenching, SPR, FRET, competition dialysis, and polymerase arrest assays) have been deployed to evaluate the relative abilities of quaternary polycyclic acridinium salts to bind to DNA isoforms, particularly duplex and quadruplex DNA. These studies have confirmed that although **8a** and **8b** possess equivalent inhibitory potencies in the TRAP assay, **8a** binds more selectively to quadruplex DNA than **8b**[12] (Table 2). In fact, the high growth-inhibitory activity of **8b** can be attributed to its indiscriminate binding to DNA, including duplex DNA[12] (Table 3). Most convincingly, over the range of compounds studied, growth-inhibitory activity (but not TRAP-inhibitory potency) correlates strongly with duplex DNA binding, whereas TRAP inhibition (but not growth-inhibitory activity) correlates with quadruplex DNA binding (Figure 7). Thus, despite the promising, rapid, in vivo antitumor efficacy of **8a**[54] and its attribution to G-quadruplex stabilization, there is no correlation between quadruplex DNA binding affinity and growth inhibition in the 2-day NCI60 growth inhibition assay. We suggest that this assay does not resolve and measure the ability of tumor cells to (re)populate a large tumor mass after the acute insult of telomere uncapping (as evidenced by rapid recruitment of the DNA damage recognition machinery at the telomeres[54]) and that alternative assays, for example, clonogenic assays,[53,54] xenografts,[54] or cumulative population doubling assessments,[53] are required to detect the relatively rapid onset of antiproliferative effects of these compounds. An example of the latter, with compound **9e**, is shown in Supporting Information (Figure S8) and has previously been shown with **8a**.[37,53,54] Furthermore, the correlations (Figure 7) confirm that SI assessment remains a valuable way of screening out compounds with high duplex DNA-associated cytotoxicity.

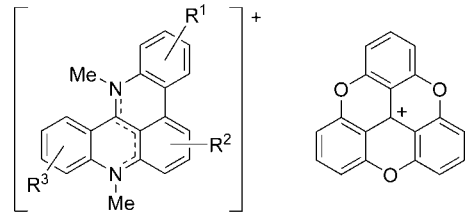

10 **11**

Figure 8. Structures of delocalized dimethylquino[4,3,2-*kl*]acridinium cations **10** and the trioxatriangulenium cation **11** depicted with charge localized at the central carbon atom.

Although the structure–activity relationships are not entirely robust, it is notable that electron-donating groups attached to the peripheral benzene rings such as methyl (**8b**), methylamino (**9c** and **9d**), and methoxyl (**9o** and **9p**) confer powerful growth-inhibitory activities in the NCI60 tumor cell screen (mean GI_{50} values of $<0.75\ \mu M$) (Table 1). Moreover, the most potent growth-inhibitory compounds **8b**, **9c**, and **9d** had mechanistic affinities with topo II inhibitors as judged by high COMPARE correlations (Table S1). In contrast, compounds with electron-withdrawing groups such as fluoro (**8a**) and acetamido (**9e** and **9n**), or bulky acryloylmorpholino substituents in the 3-, 6- or 10-positions (**9r**, **9t**, **9v**−**y**), had lower growth-inhibitory potency (range 9.33–100 μM). The structures of the quaternary quinoacridinium salts are generally depicted with positive charge localized at N-13 (see **7**−**9**). In fact, they are more accurately represented as a *delocalized* cation **10** (Figure 8). The abilities of the cation (acting as a surrogate potassium ion) to stack above or below the G-quartets as observed in NMR studies[13] is more influenced by the electronic character of appended substituents than by their steric bulk. Electron-attracting $R^1R^2R^3$ substituents in **10** (e.g., −I fluoro groups at the 3- and 11-positions in **8a**) would enhance the electron deficiency in the core of the molecule and increase its ability to bind to quadruplex DNA at the expense of other DNA isoforms. We predict that this selectivity would limit DNA duplex-associated toxicities with **8a**. Conversely, electron-donating substituents in **10** (e.g., +I methyl groups in **8b**, +M amino groups in **9b**−**d**) would reduce the electron deficiency and lead to less selective binding to quadruplex DNA. Intriguingly the trioxatriangulenium cation **11**, depicted with charge localized on the central carbon atom, also exhibits DNA quadruplex binding properties.[55] Presumably, peripheral substituents that modulate the binding of cations **10** to DNA would have similar tuning effects on cation **11**.

Compounds **8a**, **8b**, **9e**, and **9w** were also shown to generate G-quadruplex structures in a 77-mer oligonucleotide sequence incorporating a 27-mer G-rich section (Pu27) of the *c-myc* gene promoter, inferred from impediment to the polymerization of full sequence length products in favor of prematurely arrested, shorter products (Figure 6). This experiment confirms other work pointing to the potential for G-quadruplex-binding agents to engage G-rich targets other than those presented at the telomere.[31]

Conclusions

We have deduced that the isomeric quinoacridinium salts **9e** and **9n** have some noteworthy properties. They have low

growth-inhibitory activities in the NCI60 human tumor cell panel (mean GI_{50} of 12.0 and 81.3 μM, respectively), coupled with potent telomerase inhibitory activity inferred from the TRAP assay ($^{TRAP}IC_{50} < 0.5$ μM). This relates to a selectivity index (SI) of 32 and 195, respectively (Table 1), the latter value being the highest in this extensive series. In the highly sensitive SPR experiments, salts **9e** and **9n** also show the greatest differential binding affinities between duplex and quadruplex DNA (Table 3) with K being 2.4×10^7 and 2.5×10^7 M^{-1} for quadruplex DNA (cf. 0.038×10^7 and 0.044×10^7 M^{-1} for duplex DNA), making these compounds among the most selective agents yet reported.[41] We are currently exploiting these structural insights in the identification of compounds with enhanced ability to bind DNA quadruplex structures. Future in vivo studies will indicate whether or not such compounds have a unique antitumor profile with minimal collateral toxicity, either toxicity generally associated with DNA duplex-interactive agents or off (DNA)-target pharmacological activity.

Experimental Section

Chemistry. The following compounds studied in this work have been prepared previously according to the indicated references: **5**,[5] **7**,[10] **8a**−**d** and **9a**,[12] **9b**−**n**,[6] **9o**−**r**, **9t**, and **9v**−**w**,[35] and **9s**, **9u**, and **9x**−**z**.[34]

Biophysical Studies. General Procedures. Unless stated otherwise, stock solutions of compounds were prepared in DMSO (maximum final concentration, 2%) and diluted in buffer solution immediately prior to experiments. Single-stranded poly[dT], the double-stranded alternating purine−pyrimidine poly[dA-dT]·poly[dA-dT], poly[dG-dC]·poly[dG-dC] and nonalternating poly[dA]·poly[dT], poly[dG]·poly[dC] polymers, and salmon testis DNA (ST-DNA) highly polymerized sodium salt, A·T 58.8% and G·C 41.2%, were purchased from Sigma-Aldrich Chemical Co. (Dorset, England). ST-DNA was purified by ethanol precipitation. Quadruplex sequences $d[T_2G_{20}T_2]$, $d[AG_3(T_2AG_3)_3]$, and $d[T_4G_4]$, referred to as TET 1, TET 2 (human telomeric sequence), and TET 3, respectively, were purchased HPLC-purified from Sigma-Genosys (Cambridge, England) or Eurogentec (Southampton, England) and used without further purification. DNA concentrations were determined using published extinction coefficients[47,56] as follows (expressed in binding sites, bases for single stranded sequences, base pairs for double stranded, base triplets for triple stranded, and base tetrads for quadruple stranded): Poly[dT], $\lambda = 264$ nm, $\epsilon = 8520$ M^{-1} cm^{-1}; Poly[dA]*poly[dT], $\lambda = 260$ nm, $\epsilon = 12\,000$ M^{-1} cm^{-1}; Poly[dA-dT]·poly[dA-dT], $\lambda = 260$ nm, $\epsilon = 13\,100$ M^{-1} cm^{-1}; Poly[dG]·poly[dC], $\lambda = 253$ nm, $\epsilon = 14\,800$ M^{-1} cm^{-1}; Poly[dG-dC]·poly[dG-dC], $\lambda = 260$ nm, $\epsilon = 16\,800$ M^{-1} cm^{-1}; salmon testis DNA, $\lambda = 260$ nm, $\epsilon = 13\,200$ M^{-1} cm^{-1}; Poly[dT]·poly[dA]·poly[dT]: $\lambda = 260$ nm, $\epsilon = 17\,200$ M^{-1} cm^{-1}; $d[T_2G_{20}T_2]$, $\lambda = 260$ nm, $\epsilon = 39\,267$ M^{-1} cm^{-1}; $d[AG_3(T_2AG_3)_3]$, $\lambda = 260$ nm, $\epsilon = 73\,000$ M^{-1} cm^{-1}; $d[T_4G_4]$, $\lambda = 260$ nm, $\epsilon = 73\,600$ M^{-1} cm^{-1}. For quadruplex formation sequences were heated to 95 °C and then slowly cooled to room temperature over 3–4 h and stored at 4 °C. Native polyacrylamide gel electrophoresis (PAGE) was used to confirm the existence of quadruplex DNA, as was circular dichroism spectroscopy by comparing to known CD spectra of intramolecular quadruplex DNA in the literature.[57] The poly[dT]*poly[dA]·poly[dT] triplex (T*A·T) was formed by mixing a 1:1 stoichiometry of poly[dT] to poly[dA]·poly[dT] in buffer (as for UV titration below), heating to 95 °C before allowing to cool slowly to room temperature. After 18 h of equilibration at room temperature, the triplex was stored at 4 °C.

Fluorescence and UV Titration. UV absorption spectra were obtained with a Pharmacia Biotech Ultrospec 2000. Fluorescence emission spectra were measured on a Perkin-Elmer LS-5B luminescence spectrophotometer (excitation and emission slit widths of 2.5 nm); measurements were taken at λ_{max} (free drug). From a fixed volume (3 mL, 1 cm path length quartz cell) of an aqueous buffered DNA/drug solution (20:1, fluorescence; 10:1, UV; DNA concentration expressed in base pairs, drug in M^{-1}), aliquots (500 μL) were replaced by an equal volume of drug solution. This was repeated 25 times to reach an excess of drug relative to DNA. The concentration of drug remained constant throughout (3 μM, fluorescence; 20 μM, UV). Blank was aqueous buffer solution (UV, 10 mM sodium phosphate, 0.1 mM EDTA, pH 7.4; fluorescence, 185 mM NaCl, 6 mM Na_2HPO_4, 2 mM NaH_2PO_4, 0.1 mM EDTA, pH 7.0). UV absorption or fluorescence emission data points at each dilution step were plotted against DNA concentration, and the equation of Missailidis et al., 1997, was used to determine K.[38,39] The experiments were repeated three times, and the mean value was calculated.

Biosensor-Surface Plasmon Resonance (SPR) Studies. The oligonucleotides 5′-biotin-$d[AG_3(T_2AG_3)_3]$ quadruplex and 5′-biotin-d[CGCGCGCGT$_4$CGCGCGCG] duplex were purchased from Midland Certified Reagent Company (Midland, TX) with HPLC purification and mass spectrometry characterization. The concentration of each DNA sample was determined spectrophotometrically at 260 nm using the nearest-neighbor extinction coefficient. Absorbance readings at high temperature were extrapolated down to 25 °C to obtain the single-stranded absorbance for concentration calculations. A 1 mM stock solution of each compound was prepared in DMSO and diluted to working concentrations with buffer containing 1% DMSO immediately before use. The concentration of DMSO was kept constant in all diluted samples at 1%. SPR measurements were performed with a four-channel Biacore 2000 optical biosensor system (Biacore Inc.) by using published procedures.[58,59] For the quadruplex and duplex binding determinations the 5′-biotin labeled DNA samples were immobilized in separate flow cells on streptavidin-coated sensor chips (BIAcore SA) with one flow cell left blank as a control. The SPR experiments were performed at 25 °C in filtered, degassed 10 mM HEPES buffer (pH 7.4) containing 200 mM KCl, 3 mM EDTA, and 0.005% surfactant P20. Compound solutions were prepared by serial dilution from the stock solution and injected from 7 mm plastic vials with pierceable plastic crimp caps. Compound solution flow was continued until a constant steady-state response was obtained. Compound flow was then replaced by buffer flow to monitor dissociation of the complex. The reference response from the blank cell was subtracted from the response in each cell containing DNA to give a signal (RU, response units) that is directly proportional to the amount of bound compound. Sensorgrams, RU versus time, at different concentrations for binding of each compound to DNA were obtained, and the RU in the steady-state region was determined by linear averaging over a selected time span. The predicted maximum response per bound compound in the steady-state region (RU_{max}) was determined from the DNA molecular weight, the amount of DNA on the flow cell, the compound molecular weight, and the refractive index gradient ratio of the compound and DNA, as previously described.[60] The number of binding sites and the equilibrium constant were obtained from fitting plots of RU versus C_{free}.[58,59] The data were fitted to a two-site equilibrium model using Kaleidagraph for nonlinear least-squares optimization of the binding parameters:

$$RU = \frac{RU_{max}(K_1 C_{free} + 2K_1 K_2 C_{free}^{\ 2})}{(1 + K_1 C_{free} + K_1 K_2 C_{free}^{\ 2})}$$

where RU_{max} is the maximum response per bound compound and K_1 and K_2 are the macroscopic binding constants for a two-site binding model. For a single binding site model, K_2 is equal to zero.

FRET. The FRET studies were conducted according to the procedure of Mergny and co-workers in 0.1 M lithium chloride, 10 mM sodium cacodylate, pH 7.2 buffer.[45,46]

Competition Dialysis. Differential dialysis was conducted according to the procedure of Ren and Chaires,[47] using a concentration of 2 μM acridine compounds. Dialysis was carried out for 48 h at 4 °C in buffer solution (6 mM Na_2HPO_4, 2 mM NaH_2PO_4, 0.1 mM EDTA, and 185 mM NaCl, pH 7.0, supplemented with 1% SDS). The competition dialysis for each compound was performed at least three times, and the results were plotted as a mean.

Concentrations of ligand bound to the DNA were calculated using extinction coefficients for the ligands determined in the same buffer: **6**, $\lambda = 450$ nm, $\epsilon = 13\,110\ M^{-1}$; **7**, $\lambda = 505$ nm, $\epsilon = 11\,635\ M^{-1}$; **8a**, $\lambda = 510$ nm, $\epsilon = 10\,329\ M^{-1}$; **8b**, $\lambda = 512$ nm, $\epsilon = 13\,500\ M^{-1}$; **9b**, $\lambda = 495$ nm, $\epsilon = 37\,000\ M^{-1}$; **9e**, $\lambda = 514$ nm, $\epsilon = 8500\ M^{-1}$.

Enzyme Assays. Telomeric Repeat Amplification Protocol (TRAP Assay). The *Taq* DNA polymerase inhibition pre-TRAP assay screen was conducted according to a published method.[37] The TRAP assay was also conducted according to a published method[37] except that telomerase extract was prepared from A549 cells (maintained at 37 °C, humidified 95% air/5% CO_2 atmosphere in RPMI 1640 medium supplemented with L-glutamine, $NaHCO_3$, and 10% (v/v) heat-inactivated fetal bovine serum) and the assay was performed without radioactivity. Products were analyzed on a 10% native polyacrylamide gel (19:1 acrylamide/bisacrylamide in TBE buffer (890 mM Tris base, 890 mM boric acid, 2 mM EDTA), set with ammonium persulfate and TEMED); 4 μL of 6× gel loading solution (0.25% (w/v), bromophenol blue, 0.25% (w/v) xylene cyanol FF, and 40% (w/v) sucrose in water) was added to 20 μL of PCR product, and the entire 24 μL was loaded. The gel was run at 150 V for 1.5 h at 4 °C in 0.5× TBE buffer, stained with Sybr Green (1:10000 in TBE, pH 8, for 45 min, room temperature, gentle agitation) and photographed using Kodak Electrophoresis Documentation and Analysis System 120 with a SYBR Green photographic filter. Image analysis was carried out using Bio-Rad Quantity 1 software. Densitometry was used to quantify product (relative to positive control) after subtracting the densitometry score of the heat inactivated lane. Percentage of TRAP inhibition was plotted against drug concentration, and the $^{TRAP}IC_{50}$ value was interpolated from the graph. Experiments were repeated at least three times, and the mean value was calculated.

Taq Polymerase Arrest Assay. DNA sequences were obtained from Sigma-Genosys (TX). Other reagents were obtained from Sigma Chemical Co., (St. Louis, MO) unless otherwise stated. For 5′-end labeling of DNA primer, a reaction mixture of 2 μL of H_2O, 2 μL of DNA primer (2 μM) (18-mer), 1 μL of 10× T4 polynucleotide kinase reaction buffer (700 mM Tris-HCl, pH 7.6, at 25 °C, 100 mM $MgCl_2$, 50 mM DTT), 1 μL of T4 polynucleotide kinase (10u/μL) (Promega U.S., WI,) and 4 μL of [γ^{32}-P]ATP (370 MBq/mL Easytides) (Perkin-Elmer Life Sciences Inc., MA) was prepared and incubated at 37 °C for 1 h before inactivating the enzyme by heating at 90 °C for 5 min. The 5′ end-labeled primer was then isolated using a Micro Bio-Spin 6 chromatography column according to the manufacturer's instructions (Biorad Laboratories, CA), eluted in 30 μL of water, and diluted in water to the desired concentration (12 nM for the *c-myc* sequence arrest assay and 30 nM for the T2G4 sequence). The 18-mer primer had the sequence 5′-TAATACGACTCACTATAG-3′. The procedure was a modification of that already described.[31,61] A reaction mixture of template DNA (77-mer with a Pu27 insert or 73-mer with a T2G4 insert; see below) (50 nM for the Pu27 insert, 10 nM for T2G4), Tris-HCl (50 mM), $MgCl_2$ (10 mM), DTT (0.5 mM), EDTA (0.1 mM), BSA (60 ng), and γ-^{32}P 5′-end labeled 18-mer primer (12 nM for Pu27 insert, 30 nM for T2G4) was denatured by heating to 90 °C for 5 min and then allowed to cool to 60 °C over 30 min and placed at ambient temperature for 20 min to allow quadruplex formation; 8 μL of reaction mixture and 1 μL of compound (10× final concentration desired, ranging from 0.01 to 100 μM) were then mixed and preincubated at room temperature for 30 min to allow the compounds to interact with the quadruplex. A drug-free control was prepared with water in place of 10× drug. The primer-extension reactions were initiated by adding 1 μL of Taq DNA polymerase (Promega U.S., WI) in storage buffer containing 100 mM KCl to each reaction mixture (giving a final KCl concentration of 10 mM), and the mixtures were maintained at 55 °C for 30 min. A Taq polymerase-free negative control was also included. Following the addition of an equal volume of 2× arrest buffer (95% formamide, 10 mM EDTA, 10 mM NaOH, 0.1% xylene cyanol, 0.1% bromophenol blue), the products were denatured by heating to 90 °C for 5 min and separated on a 12% denaturing gel (see below). The sequence for the 77-mer template with the Pu27 insert was 5′-TCCAACTATGTATAC-insert-TTAGCGACACGCAATTGC-TATAGTGAGTCGTATTA-3′. The sequence of the Pu27 insert was 5′-TGGGGAGGGTGGGGAGGGTGGGGAAGG-3′. The sequence for the 73-mer template with the T2G4 insert was 5′-TCCAACTATGTATAC-insert-TTAGCGGCACGCAATTGCTAT-AGTGAGCGTATTA-3′, and the sequence of the T2G4 insert was 5′-TTGGGGTTGGGGTTGGGGTTGGGG-3′. Gels were prepared from a stock solution of the following components: 230 g of urea, 150 mL of 40% acrylamide/bisacrylamide solution, 50 mL of 10× TBE buffer made up to 500 mL with deionized water. Polymerization agents (600 μL of 10% APS, 30 μL of TEMED) were added to 100 mL, and the gel was poured between glass plates separated with a 0.3 mm spacer. The gel was allowed to set for 30 min and then prerun with 1× TBE buffer at 2000 V for 30 min before loading and running at 1900 V for 2 h (Life Technologies Gibco BRL sequencing system model S2 electrophoresis apparatus, EC Apparatus Powerpack series 90 programmable EC400P). The gel was dried between sheets of Whatman 3MM filter paper at 80 °C for 45 min (Biorad gel dryer model 583) and visualized on a Molecular Dynamics Storm 860 PhosphorImager. For quantification, the intensity of the bands representing the full length product (77-mer) and the proposed G-quadruplex arrest site was determined using ImageQuant software.

Acknowledgment. We thank S. M. Gowan and L. R. Kelland at the Institute of Cancer Research in Sutton, U.K., for conducting some of the TRAP assays. Taq polymerase arrest assays were conducted at the Arizona Cancer Centre, Tucson, AZ. We thank L. H. Hurley for supervising this work and for supplies of TMPyP4. Work in Nottingham was supported by grants from Cancer Research U.K.

Supporting Information Available: Additional biophysical and biological data relating to the polycyclic acridine series described in this paper. This material is available free of charge via the Internet at http://pubs.acs.org.

References

(1) Part 19: Hutchinson, I.; Stevens, M. F. G. Synthetic strategies to a telomere-targeted pentacyclic heteroaromatic salt. *Org. Biomol. Chem.* **2007**, *5*, 114–120.

(2) Fugman, B.; Steffan, B.; Steglich, W. Necatarone, an alkaloidal pigment from the gilled toadstool *Lactarius necator* (*Agaicales*). *Tetrahedron Lett.* **1984**, *25*, 3575–3578.

(3) (a) Hagan, D. J.; Giménez-Arnau, E.; Schwalbe, C. H.; Stevens, M. F. G. Antitumour polycyclic acridines. Part 1. Synthesis of 7*H*-pyrido- and 8*H*-quino[4,3,2-*kl*]acridines by Graebe−Ullmann thermolysis of 9-(1,2,3-triazol-1-yl)acridines: application of differential scanning calorimetry to predict optimum cyclisation conditions. *J. Chem. Soc., Perkin Trans. 1* **1997**, 2739–2746. (b) Hagan, D. J.; Chan, D.; Schwalbe, C. H.; Stevens, M. F. G. Antitumour polycyclic acridines. Part 3. A two-step conversion of 9-azidoacridine to 7*H*-pyrido[4,3,2-*kl*]acridines by Graebe−Ullmann thermolysis of substituted 9-(1,2,3-triazol-1-yl)acridines. *J. Chem. Soc., Perkin Trans. 1* **1998**, 915–923. (c) Julino, M.; Stevens, M. F. G. Antitumour polycyclic acridines. Part 5. Syntheses of 7*H*-pyrido[4,3,2-*kl*]acridines with exploitable functionality in the pyridine ring. *J. Chem. Soc., Perkin Trans. 1* **1998**, 1677–1684. (d) Ellis, M. J.; Stevens, M. F. G. Antitumour polycyclic acridines. Part 9. Synthesis of 7*H*-pyrido[4,3,2-*kl*]acridines with basic side chains. *J. Chem. Soc., Perkin Trans. 1* **2001**, 3174–3179.

(4) Stanslas, J.; Hagan, D. J.; Ellis, M. J.; Turner, C.; Carmichael, J.; Ward, W.; Hammonds, T. R.; Stevens, M. F. G. Antitumor polycyclic acridines. 7. Synthesis and biological properties of DNA affinic tetra- and pentacyclic acridines. *J. Med. Chem.* **2000**, *43*, 1563–1572.

(5) Ellis, M. J.; Stevens, M. F. G. Antitumour polycyclic acridines. Part 10. Synthesis of penta- and hexa-cyclic heteroaromatic systems by radical cyclisations of substituted 9-anilinoacridines. *J. Chem. Soc., Perkin Trans. 1* **2001**, 3180–3185.

(6) Hutchinson, I.; McCarroll, A. J.; Heald, R. A.; Stevens, M. F. G. Synthesis and properties of bioactive 2- and 3-amino-8-methyl-8*H*-quino[4,3,2-*kl*]acridine and 8,13-dimethyl-8*H*-quino[4,3,2-*kl*]acridinium salts. *Org. Biomol. Chem.* **2004**, *2*, 220–228.

(7) Shoemaker, R. H. The NCI60 human tumour cell line anticancer drug screen. *Nat. Rev. Cancer* **2006**, *6*, 813–823.

(8) Albert, A. *The Acridines*, 2nd ed.; Edward Arnold: London, 1966.
(9) Bostock-Smith, C. E.; Giménez-Arnau, E.; Missailidis, S.; Laughton, C. A.; Stevens, M. F. G.; Searle, M. S. Molecular recognition between a new pentacyclic acridinium salt and DNA sequences investigated by optical spectroscopic techniques, proton nuclear magnetic resonance spectroscopy and molecular modeling. *Biochemistry* **1999**, *38*, 6723–6731.
(10) Ozczapowicz, D.; Jaroszewska-Manaj, J.; Ciszak, E.; Gdaniec, M. Formation of quinoacridinium system. A novel reaction of quinaldinium salts. *Tetrahedron* **1988**, *44*, 6645–6650.
(11) Missailidis, S.; Stanslas, J.; Modi, C.; Ellis, M. J.; Robins, R. A.; Laughton, C. A.; Stevens, M. F. G. Antitumour polycyclic acridines. Part 12. Physical and biological properties of 8,13-diethyl-6-methylquino[4,3,2-*kl*]acridinium iodide: a lead compound in anti-cancer drug design. *Oncol. Res.* **2002**, *13*, 175–189.
(12) Heald, R. A.; Modi, C.; Cookson, J. C.; Hutchinson, I.; Laughton, C. A.; Gowan, S. M.; Kelland, L. R.; Stevens, M. F. G. Antitumor polycyclic acridines. 8. Synthesis and telomerase-inhibitory activity of methylated pentacyclic acridinium salts. *J. Med. Chem.* **2002**, *45*, 590–597.
(13) (a) Gavathiotis, E.; Heald, R. A.; Stevens, M. F. G.; Searle, M. S. Recognition and stabilization of quadruplex DNA by a potent new telomerase inhibitor: NMR studies of the 2:1 complex of a pentacyclic methylacridinium cation with d(TTAGGGT)$_4$. *Angew. Chem., Int. Ed.* **2001**, *40*, 4749–4751. (b) Gavathiotis, E.; Heald, R. A.; Stevens, M. F. G.; Searle, M. S. Drug recognition and stabilization of the parallel-stranded DNA quadruplex d(TTAGGGT)$_4$ containing the human telomeric repeat. *J. Mol. Biol.* **2003**, *334*, 25–36.
(14) Phan, T. P.; Kuryavyi, V.; Patel, D. J. DNA architecture: from G to Z. *Curr. Opin. Struct. Biol.* **2006**, *16*, 288–298.
(15) Huppert, J. L.; Subramanian, S. Prevalence of quadruplexes in the human genome. *Nucleic Acids Res.* **2005**, *33*, 2908–2916.
(16) Moyzis, R. K.; Buckingham, J. M.; Cram, L. S.; Dani, M.; Deaven, L. L.; Jones, M. D.; Meyne, J.; Ratliff, R. L.; Wu, J. R. A highly conserved repetitive DNA sequence, (TTAGGG)$_n$, present at the telomeres of human chromosomes. *Proc. Natl. Acad. Sci. U.S.A.* **1988**, *85*, 6622–6626.
(17) (a) Blackburn, E. H. Structure and function of telomeres. *Nature* **1991**, *350*, 569–573. (b) Blackburn, E. H. Telomere states and cell fates. *Nature* **2000**, *408*, 53–56.
(18) Wang, Y.; Patel, D. J. Solution structure of the human telomeric repeat d[AG$_3$(T$_2$AG$_3$)$_3$] G-tetraplex. *Structure* **1993**, *1*, 263–282.
(19) Parkinson, G. N.; Lee, M. P. H.; Neidle, S. Crystal structure of parallel quadruplexes from human telomeric DNA. *Nature* **2002**, *417*, 876–880.
(20) (a) Luu, K. N.; Phan, A. T.; Kuryavyi, V.; Lacroix, L.; Patel, D. J. Structure of the human telomere in K^+ solution: an intramolecular (3+1) G-quadruplex scaffold. *J. Am. Chem. Soc.* **2006**, *128*, 9963–9970. (b) Ambrus, A.; Chen, D.; Dai, J.; Bialis, T.; Jones, R. A.; Yang, D. Human telomeric sequence forms a hybrid-type intramolecular G-quadruplex structure with mixed parallel/antiparallel strands in potassium solution. *Nucleic Acids Res.* **2006**, *34*, 2723–2735.
(21) Zahler, A. M.; Williams, J. R.; Cech, T. R.; Prescott, D. M. Inhibition of telomerase by G-quartet DNA structures. *Nature* **1991**, *350*, 718–720.
(22) Kim, N. W.; Piatyszek, M. A.; Prowse, K. R.; Harley, C. B.; West, M. D.; Ho, P. L. C.; Coviello, G. M.; Wright, W. E.; Weinrich, S. L.; Shay, J. W. Specific association of human telomerase activity with immortal cells and cancer. *Science* **1994**, *266*, 2011–2015.
(23) Hahn, W. C.; Stewart, S. A.; Brooks, M. W.; York, S. G.; Eaton, E.; Kurachi, A.; Beijersbergen, R L.; Knoll, J. H. M.; Meyerson, M.; Weinberg, R. A. Inhibition of telomerase limits the growth of human cancer cells. *Nat. Med.* **1999**, *5*, 1164–1170.
(24) Shay, J. W.; Wright, W. E. Telomerase therapeutics for cancer: challenges and new directions. *Nat. Rev. Drug Discovery* **2006**, *5*, 577–584.
(25) (a) Kelland, L. R. Overcoming the immortality of tumour cells by telomere and telomerase based cancer therapeutics—current status and future prospects. *Eur. J. Cancer* **2005**, *41*, 971–979. (b) Neidle, S.; Parkinson, G. Telomere maintenance as a target for anticancer drug discovery. *Nat. Rev. Drug Discovery* **2002**, *1*, 383–393.
(26) (a) Giraldo, R.; Rhodes, D. The yeast telomere-binding protein RAP1 binds to and promotes the formation of DNA quadruplexes in telomeric DNA. *EMBO J.* **1994**, *13*, 2411–2420. (b) Muniyappa, K.; Anuradha, S.; Byers, B. Yeast meiosis-specific protein Hop 1 binds to G4 DNA and promotes its formation. *Mol. Cell. Biol.* **2000**, *20*, 1361–1369.
(27) (a) Liu, Z.; Gilbert, W. The yeast KEM1 gene encodes a nuclease specific for G4 tetraplex DNA: implication of in vivo functions for this novel DNA structure. *Cell* **1994**, *77*, 1083–1092. (b) Sun, H.; Yabuki, A.; Maisels, N. A human nuclease specific for G4 DNA. *Proc. Natl. Acad. Sci. U.S.A.* **2001**, *98*, 12444–12449.
(28) Li, J.-L.; Harrison, R. J.; Reszka, A. P. ; Brosh, R. M. Jr.; Bohr, V. A.; Neidle, S.; Hickson, D. Inhibition of the Bloom's and Werner's syndrome helicases by G-quadruplex interacting ligands. *Biochemistry* **2001**, *40*, 15194–15202.
(29) (a) Schaffitzel, C.; Berger, I.; Postberg, J.; Hanes, J.; Lipps, H. J.; Pluckthun, A. In vitro generated antibodies specific for telomeric guanine-quadruplex DNA react with *Stylonychia lemnae* macronuclei. *Proc. Natl. Acad. Sci. U.S.A.* **2001**, *98*, 8572–8577. (b) Paeschke, K.; Simonsson, T.; Postberg, J.; Rhodes, D.; Lipps, H. J. Telomere end-binding proteins control the formation of G-quadruplex DNA structures in vivo. *Nat. Struct. Mol. Biol.* **2005**, *12*, 847–854.
(30) Simonsson, T. G-quadruplex DNA structures—variations on a theme. *Biol. Chem.* **2001**, *382*, 621–628.
(31) Siddiqui-Jain, A.; Grand, C. L.; Bearss, D. J.; Hurley, L. H. Direct evidence for a G-quadruplex in a promoter region and its targeting with a small molecule to repress c-MYC Transcription. *Proc. Natl. Acad. Sci. U.S.A.* **2002**, *99*, 11593–11598.
(32) Mergny, J.-L.; Riou, J.-F.; Mailliet, P.; Teulade-Fichou, M.-P.; Gilson, E. Natural and pharmacological regulation of telomerase. *Nucleic Acids Res.* **2002**, *30*, 839–865.
(33) (a) Leonetti, C.; Amodei, S.; D'Angelo, C.; Rizzo, A.; Benassi, B.; Antonelli, A.; Elli, R.; Stevens, M.; D'Incalci, M.; Zupi, G.; Biroccio, A. Biological activity of the G-quadruplex ligand RHPS4 (3,11-difluoro-6,8,13-trimethyl-8*H*-quino[4,3,2-*kl*]acridinium methosulfate) is associated with telomere capping alteration. *Mol. Pharmacol.* **2004**, *66*, 1138–1146. (b) Biroccio, A.; Rizzo, A.; Elli, R.; Koering, C.-E.; Belleville, A.; Benassi, B.; Leonetti, C.; Stevens, M.; D'Incalci, M.; Zupi, G.; Gilson, E. TRF2 inhibition triggers apoptosis and reduces tumourigenicity of human melanoma cells. *Eur. J. Cancer* **2006**, *42*, 1881–1888.
(34) Cookson, J. C.; Heald, R. A.; Stevens, M. F. G. Antitumor polycyclic acridines. 17. Synthesis and pharmaceutical profiles of pentacyclic acridinium salts designed to destabilize telomeric integrity. *J. Med. Chem.* **2005**, *48*, 7198–7207.
(35) Heald, R. A.; Stevens, M. F. G. Antitumour polycyclic acridines. Palladium(0) mediated syntheses of quino[4,3,2-*kl*]acridines bearing peripheral substituents as potential telomere maintenance inhibitors. *Org. Biomol. Chem.* **2003**, *1*, 3377–3389.
(36) Weinstein, J. N.; Myers, T. G.; O'Connor, P. M.; Friend, S. H.; Fornace, A. J.; Kohn, K. W.; Fojo, T.; Bates, S.; Rubenstein, V.; Anderson, N. L.; Buolamwini, J. K.; Van Osdol, W. W.; Monks, A.; Scuderio, D. A.; Sausville, E. A.; Zaharevitz, D. W.; Bunow, B.; Viswanadhan, V. N.; Johnson, G. S.; Wittes, R. E.; Paull, K. D. An information-intensive approach to the molecular pharmacology of cancer. *Science* **1997**, *275*, 343–349.
(37) Gowan, S. M.; Heald, R.; Stevens, M. F. G.; Kelland, L. R. Potent inhibition of telomerase by small molecule pentacyclic acridines capable of interacting with G-quadruplexes. *Mol. Pharmacol.* **2001**, *60*, 981–988.
(38) Missailidis, S.; Cannon, W. V.; Drake, A.; Wang, X. Y.; Buck, M. Analysis of the architecture of the transcription factor sigma N (sigma54) and its domains by circular dichroism. *Mol. Microbiol.* **1997**, *24*, 653–664.
(39) (a) Giménez-Arnau, E.; Missailidis, S.; Stevens, M. F. G. Antitumour polycyclic acridines. Part 2. Physico-chemical studies on the interactions between DNA and novel polycyclic acridine derivatives. *Anti-Cancer Drug Des.* **1998**, *13*, 125–413. (b) Giménez-Arnau, E.; Missailidis, S.; Stevens, M. F. G. Antitumour polycyclic acridines. Part 4. Physico-chemical studies on the interactions between DNA and novel tetracyclic acridine derivatives. *Anti-Cancer Drug Des.* **1998**, *13*, 431–451.
(40) Record, M. T.; Anderson, C. F.; Lohman, T. M. Thermodynamic analysis of ion effects on the binding and conformational equilibria of proteins and nucleic acids: the roles of ion association or release, screening, and ion effects on water activity. *Q. Rev. Biophys.* **1978**, *11*, 103–178.
(41) White, E. W.; Tanious, F.; Ismail, M. A.; Reszka, A. P.; Neidle, S.; Boykin, D. W.; Wilson, W. D. Structure-specific recognition of quadruplex DNA by organic cations: influence of shape, substituents and charge. *Biophys. Chem.* **2007**, *126*, 140–153.
(42) McDonnell, J. M. Surface plasmon resonance: towards an understanding of the mechanisms of biological molecular recognition. *Curr. Opin. Chem. Biol.* **2001**, *5*, 572–577.
(43) Harrison, R. J.; Cuesta, J.; Chessari, G.; Read, M. A.; Basra, S. K.; Reszka, A. P.; Morrell, J.; Gowan, S. M.; Incles, C. M.; Tanious, F. A.; Wilson, W. D.; Kelland, L. R.; Neidle, S. Trisubstituted acridine derivatives as potent and selective telomerase inhibitors. *J. Med. Chem.* **2003**, *46*, 4463–4476.
(44) Teulade-Fichou, M.-P.; Carrasco, C.; Guittat, L.; Bailly, C.; Alberti, P.; Mergny, J.-L.; David, A.; Lehn, J. M.; Wilson, W. D. Selective recognition of G-quadruplex telomeric DNA by a bis(quinacridine) macrocycle. *J. Am. Chem. Soc.* **2003**, *125*, 4732–4740.
(45) Mergny, J.-L.; Lacroix, L.; Teulade-Fichou, M.-P.; Hounsou, C.; Guittat, L.; Hoarau, M.; Arimondo, P. B.; Vigneron, J.-P.; Lehn, J.-

M.; Riou, J.-F.; Montenay-Garestier, T.; Hélène, C. Telomerase inhibitors based on quadruplex ligands selected by a fluorescence assay. *Proc. Natl. Acad. Sci. U.S.A.* **2001**, *98*, 3062–3067.
(46) De Cian, A.; Guittat, L.; Kaiser, M.; Saccà, B.; Amrane, S.; Bourdoncle, A.; Alberti, P.; Teulade-Fichou, M.-P.; Lacroix, L.; Mergny, J.-L. Fluorescence-based melting assays for studying quadruplex ligands. *Methods* **2007**, *42*, 183–195.
(47) (a) Ren, J.; Chaires, J. B. Sequence and structural selectivity of nucleic acid binding ligands. *Biochemistry* **1999**, *38*, 16067–16075. (b) Ren, J.; Chaires, B. Rapid screening of structurally selective ligand binding to nucleic acids. *Methods Enzymol.* **2001**, *340*, 99–108.
(48) Harrison, R. J.; Gowan, S.; Kelland, L. R.; Neidle, S. Human telomerase inhibition by substituted acridine derivatives. *Bioorg. Med. Chem. Lett.* **1999**, *9*, 2463–2468.
(49) (a) Schultes, C. M.; Guyen, B.; Cuesta, J.; Neidle, S. Synthesis, biophysical and biological evaluation of 3,6-bis-amidoacridines with extended 9-anilino substituents as potent G-quadruplex-binding telomerase inhibitors. *Bioorg. Med. Chem. Lett.* **2004**, *14*, 4347–4351. (b) Incles, C. M.; Schultes, C. M.; Kempski, H.; Koehler, H.; Kelland, L. R.; Neidle, S. A G-quadruplex telomere targeting agent produces p16-associated senescence and chromosomal fusions in human prostate cancer cells. *Mol. Cancer Ther.* **2004**, *3*, 1201–1206.
(50) (a) Izbicka, E.; Nishioka, D.; Marcell, V.; Raymond, E.; Davidson, K. D.; Lawrence, R. A.; Wheelhouse, R. T.; Hurley, L. H.; Wu, R. S.; Von Hoff, D. D. Telomere-interactive agents affect proliferation rates and induce chromosomal destabilization in sea urchin embryos. *Anti-Cancer Drug Des.* **1999**, *14*, 355–365. (b) Izbicka, E.; Wheelhouse, R. T.; Raymond, E.; Davidson, K. D.; Lawrence, R. A.; Windle, B. E.; Hurley, L. H.; Von Hoff, D. D. Effects of cationic porphyrins as G-quadruplex interactive agents in human tumour cells. *Cancer Res.* **1999**, *59*, 639–644.
(51) Riou, J.-F.; Guittat, L.; Mailliet, P.; Laoui, A.; Renou, E.; Petitgenet, O.; Mégnin-Chanet, F.; Hélène, C.; Mergny, J.-L. Cell senescence and telomere shortening by a new series of specific G-quadruplex DNA ligands. *Proc. Natl. Acad. Sci. U.S.A.* **2002**, *99*, 2672–2677.
(52) Karlseder, J.; Smogorzewska, A.; de Lange, T. Senescence induced by altered telomere state, not telomere loss. *Science* **2002**, *295*, 2446–2449.
(53) Cookson, J. C.; Dai, F.; Smith, V.; Heald, R. A.; Laughton, C. A.; Stevens, M. F. G.; Burger, A. M. Pharmacodynamics of the G-quadruplex-stabilizing telomerase inhibitor 3,11-difluoro-6,8,13-trimethyl-8*H*-quino[4,3,2-*kl*]acridinium methosulfate (RHPS4) in vitro: activity in human tumor cells correlates with telomere length and can be enhanced, or antagonized, with cytotoxic agents. *Mol. Pharmacol.* **2005**, *68*, 1551–1558.
(54) Salvati, E.; Leonetti, C.; Rizzo, A.; Scarsella, M.; Mottolese, M.; Galati, R.; Sperduti, I.; Stevens, M.; D'Incalci, M.; Blasco, M.; Chiorino, G.; Bauwens, S.; Horard, B.; Gilson, E.; Stoppacciaro, A.; Zupi, G.; Biroccio, A. Telomere damage induced by the G-quadruplex ligand RHPS4 has an antitumor effect. *J. Clin. Invest.* **2007**, *117*, 3236–3247.
(55) Pothukuchy, A.; Mazzitelli, C. L.; Rodriguez, M. L.; Tuesuwan, B.; Salazar, M.; Brodbelt, J. S.; Kerwin, S. M. Duplex and quadruplex DNA binding and photocleavage by trioxatriangulenium ion. *Biochemistry* **2005**, *44*, 2163–2172.
(56) (a) Jenkins, T. C. Optical absorbance and fluorescence techniques for measuring DNA−drug interactions. *Methods Mol. Biol.* **1997**, *90*, 195–218. (b) Haq, I.; Trent, J. O.; Chowdhry, B. Z.; Jenkins, T. C. Intercalative G-tetraplex stabilization of telomeric DNA by a cationic porphyrin. *J. Am. Chem. Soc.* **1999**, *121*, 1768–1779.
(57) Balagurumoorthy, P.; Brahmachari, S. K. Structure and stability of human telomeric sequence. *J. Biol. Chem.* **1994**, *269*, 21858–21869.
(58) Moore, M. J.; Schultes, C. M.; Cuesta, J.; Cuenca, F.; Gunaratnam, M.; Tanious, F. A.; Wilson, W. D.; Neidle, S. Trisubstituted acridines as G-quadruplex telomere targeting agents. Effects of extensions of the 3,6- and 9-side chains on quadruplex binding, telomerase activity, and cell proliferation. *J. Med. Chem.* **2006**, *49*, 582–599.
(59) Rezler, E. M.; Seenisamy, J.; Bashyam, S.; Kim, M. Y.; White, E.; Wilson, W. D.; Hurley, L. H. Telomestatin and diseleno sapphyrin bind selectively to two different forms of the human telomeric G-quadruplex structure. *J. Am. Chem. Soc.* **2005**, *127*, 9439–9447.
(60) Davis, T. M.; Wilson, W. D. Determination of the refractive index increments of small molecules for correction of surface plasmon resonance data. *Anal. Biochem.* **2000**, *284*, 348–353.
(61) Weitzmann, M. N.; Woodford, K. J.; Usdin, K. The development and use of a DNA polymerase arrest assay for the evaluation of parameters affecting intrastrand tetraplex formation. *J. Biol. Chem.* **1996**, *271*, 20958–20964.

JM070587T